



# Evaluating the Effects of Gas Tungsten Arc Weld Parameters on Mechanical Properties of UNS S31803 Stainless Steel Weldment

Uchendu I. Frank, Macauley T. Lilly, Morrison V. Ndor, and Felix E. Oparadike  
Department of Mechanical Engineering, Rivers State University, Port Harcourt, Nigeria.

[uchenduimereoma@yahoo.com](mailto:uchenduimereoma@yahoo.com)

## ABSTRACT:

The focus of this study was to evaluate the weld parameters in relation to heat input and their effect on corrosion and mechanical properties. Such properties include hardness, tensile strength and impact toughness of UNS S31803 stainless steel. Using the process of Gas Tungsten Arc Weld, samples of 50.8mm (2inch) UNS S31803 stainless steel pipe with dimensions of thickness 5.54mm and 300mm length were welded. The range of parameters in which the weld was carried out are voltage of 10-12V, speed of weld 50-90mm/min, and weld current 100-150A. To ensure no defects, samples were first tested non-destructively after welding and micro-structural examinations and ferrite content measurements were performed. Corrosion test, according to ASTM G48 standard, was conducted. The heat input effect on hardness, tensile, and impact toughness was also examined. The effects of the parameters were studied from the experiment results. It was observed that there were improved mechanical properties at low heat input than high heat input. The Corrosion rate for optimized parameters at 22°C and 28°C were 0.04g/m<sup>2</sup>.day, and 0.74g/m<sup>2</sup>.day respectively, which is lower than the 1.00g/m<sup>2</sup>.day in which corrosion is said to be initiated. The optimum welding parameters of the experiment were found to be welding current of 100A, voltage of 10V, and speed of 90mm/min. The hardness, tensile strength and impact toughness values for the optimized parameters after conducting a confirmation experiment were found to be 371HVN, 994MPa, and 237J respectively. The study showed that weldment has higher strength values than the base metal.

**KEYWORDS:** Austenite, Heat, Ferrite, V-notch, Weld.

**Cite This Article:** Frank, U. I., Lilly, M. T., Ndor, M. V. and Oparadike, F. E. (2020). Evaluating the Effects of Gas Tungsten Arc Weld Parameters on Mechanical Properties of UNS S31803 Stainless Steel Weldment. *Journal of Newviews in Engineering and Technology (JNET)*, 2 (1), 84-96.

## 1. INTRODUCTION:

The establishment of duplex stainless steel was about 75 years ago, but there were still problems encountered in the austenite-ferrite equilibrium.

Originally these steels were produced as substitutes of low nickel to austenite stainless steel in use wherever the resistance to decomposition, joining capability, and strength capability are of high concern. In recent world of infrastructural modernization and industrialization the wear, in form of abrasion and corrosion, is creating a huge challenge that is worth millions of naira. UNS 31803 steel has high strength and high resistance to corrosion. However, it also undergoes many corrosion deformations and mechanical properties deterioration in environments such as chloride solutions that are aggressive on metals. When welding, the protection of weld pool from the environment is the main problem encountered. The oxygen detrimental effects on the properties of weld metal (in the form of oxide inclusions of weld metal) are known by researchers. Properties like toughness and weld plasticity are severely affected (Potapov, 1993).

The combination of good mechanical properties, resistance to corrosion, relatively low cost and maintenance has been the attributes to the wide spread usage of stainless steels in engineering applications. However, welding of stainless steel (a process that is essential in many industries) has experienced a number of problems. In spite of the fact that efforts have been made to improve weld qualities of stainless steels and susceptibility to hot cracking, impediments are still related with weld properties, especially welding of component that needs multi-pass weld. The heat-affected zone (HAZ) as well as different weld passes is subject to variable heat cycles with the placement of each subsequent pass which can lead to the occurrence of complex changes in microstructure.

One of the major issues for service life increment and reliability of metallic materials is corrosion, and detailed knowledge and understanding of its mechanism is vital to solving the existing and future problem of corrosion (Marcus, 2002). Corrosion can simply be defined as the electrochemical reaction on the surface of metal which results to degradation (Trethewey & Chamberlain, 1995). Its process is natural and it is as a result of the metal tendency to get to the lowest energy state. To attain that level, for example, combining steel and iron with water and oxygen for the formation of hydrated iron oxide (rust) which is similar to that of iron ore (Davis, 2006). See figure 1 showing the life cycle of steel.

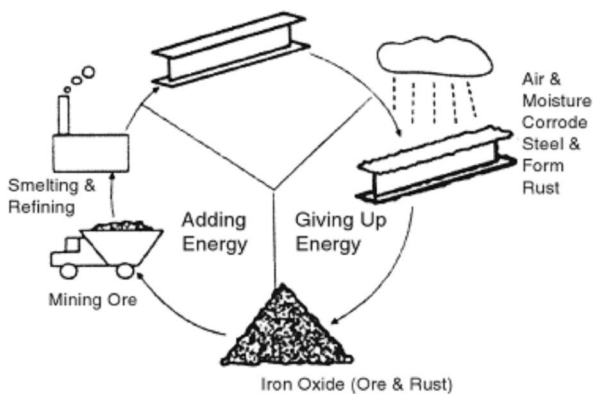


Figure 1: Life Cycle of Steel (Elena, 2014)

Generally, stainless steels are highly resistant to corrosion and satisfactorily perform in many environments. The constituent element of a given stainless steel determines its limit of corrosion resistance, which means that each grade, when exposed to an environment that is corrosive, has a response that is slightly different from another. Hence, carefulness is required when selecting the most suitable grade of stainless steel for a given application. Also, careful selection of material grade, workmanship and good detailing can significantly reduce the likelihood of corrosion and staining.

Stainless steel is made by the combination of carbon steel with other alloying elements, such as nickel, manganese, titanium, aluminum, silicon, copper, and chromium. The elements are added in different proportions in order for the material to take a different aspect like strength increase, increase in resistance to corrosion, enhanced formability or ductility, change in the weld ability.

Corrosion failure of welds can still occur regardless of the fact that the proper filler metal and parent metal have been selected; standards and industry codes followed, and welds that possess full weld penetration deposited and have good contour and shape. Although, the parent form of a stainless steel may be corrosion resistant in a particular environment, the weld counterpart is not. There are instances where the weld exhibits high resistance to corrosion than that of the welded base metal. Also, the weld can behave in an erratic manner, displaying both resistance and susceptibility to corrosive attack.

Pardal *et al.* (2011) determined the characterization and evaluation of corrosion resistance of welded joint of duplex stainless-steel pipe UNS S31803 by submerged Arc process. This study presents the corrosion resistance, micro-structural, and mechanical properties of a duplex stainless-steel welded joint of pipe wall thickness of 35mm. The results of chemical composition, mechanical properties and corrosion resistance characterization in different regions of the welded joint were compared to the base and to the specifications required by the standards applied in the project.

Hynn *et al.* (2017) evaluated the characteristics of duplex stainless steel UNS S31803 weldment made with FCAW in terms of micro-structure, ferrite content, EDS and XRD analysis, hardness, tensile strength, impact toughness, and pitting corrosion



resistance. It was observed that hardness of the weld metal was improved than that of the base metal, and the least amount of pitting corrosion occurred in heat input 12.5kJ/cm.

Verma *et al.* (2019) studied the evaluation of metallurgical phases and its co-relation with mechanical properties and corrosion resistance of 22Cr–5Ni–3M<sub>o</sub> and 16Cr–10Ni–2M<sub>o</sub> dissimilar weldment. This study addressed the dissimilar weld between 22Cr–5Ni–3M<sub>o</sub> and 16Cr–10Ni–2M<sub>o</sub> stainless steel, applying Submerge Metal Arc Weld (SMAW) process by the use of two different welding parameters (based on current) and investigated the micro-structural evolution, and correlated with the mechanical properties and corrosion resistance of the weldments. It was observed that increase in heat input decreases the ferritic content of the welded region resulting in decreased hardness and tensile strength.

Zhang *et al.* (2017) investigated the influence of heat input in electron beam weld (EBW) process on microstructure, mechanical properties and pitting corrosion resistance of duplex stainless-steel welded interface. It is stated in the result of this study that an increased heat input promotes grain boundary austenite growth and the formation of fine intergranular austenite, and the microhardness of the EB weldment significantly higher than that of the base metal.

Paulraj and Garg (2016) investigated the effect of welding parameters on pitting behaviour of GTAW of Duplex Stainless Steel (DSS) and super DSS weldments. Parameters such as inter-pass temperature, shielding/back-purging gas, heat input, and cooling rate were used to determine the corrosion behaviour of DSS and super DSS stainless steel. It was concluded, based on the experiment conducted, that improved corrosion properties were observed at low heat input,

low inter-pass temperature, higher nitrogen content in shielding/back purging gas, and faster cooling rate

It has been discovered that enough or thorough investigation have not been done by considering the welding parameters such as the weld current, weld voltage, and weld speed of GTAW of UNS S31803 stainless steel. The main aim of this research is to characterize the corrosion behavior and mechanical properties of UNS S31803 stainless steel pipe using the GTAW technique which is commonly used in welding of UNS S31803. The objectives of this work are to: Investigate the performances of the Gas Tungsten Arc Weld (GTAW) process on the UNS S31803 specimens; conduct an analysis on the microstructure of the various weld-passes in terms of phase transformation; determine the rate of corrosion by performing a corrosion test on weldment using the ASTM standard; determine the mechanical properties of weldments by conducting mechanical tests such as the tensile test, hardness test, and impact toughness test; determine the most effective parameters in the process by using the Taguchy method of data analysis; and conduct a confirmation experiment on the optimized parameter of the analysis.

## 2. MATERIALS AND METHODS:

### 2.1 Materials

The materials for this research were samples of 50.8mm (2 inch) UNS 31803 duplex stainless-steel pipe with 5.54mm thickness and 300mm length. Figure 3 shows the image of welded samples used in the experiment. It has been considered to be a good representative in the family of duplex stainless steel. The welding filler metal used for welding is of specification according to the British standard BS EN 1600 (22.9.3 NL) with a diameter of 1.2mm. This is preferred in so as to have a filler metal that is convenient for the weld current range. This steel has been widely used in many industries where



components or pipes are subjected to highly aggressive composition of UNS 31803 base metal and filler metal environments. See Tables 1 and 2 for chemical (22.9.3 NL) respectively.

**Table 1: Chemical Composition of Base Material (UNS 31803) PREN = 34.47**

Element	C	Si	Cr	Ni	P	Mn	N	S	Mo
Composition, w%	0.03	1.00	22.00	4.50	0.03	2.00	0.14	0.02	2.50

**Table 2: Chemical Composition of Filler Metal Material (22.9.3 NL)**

Element	C	Si	Mn	Cr	Ni	Mo	N
Composition, w%	0.015	0.400	1.700	22.500	8.800	3.200	0.150

## 2.2 Procedures

GTAW process was used in welding the UNS S31803 pipes. The welding process was performed at the fabrication workshop of Aveon Offshore Limited, Port Harcourt. The welding was carried out within the range of parameters defined in the Table 3.

The changes in fusion or parameters of arc weld leads to welding heat input variations. Varying the input of heat typically affects the microstructure and mechanical properties of the weld (Funderburk, 1999). The welding heat input per unit length of weld can be calculated using equation 1.

$$\text{Heat input, } H(\text{J/mm}) = \frac{60 \times VI}{S} \quad (1)$$

Where

V	=	Arc voltage, V
I	=	Welding current, A
S	=	Welding speed, mm/min

Each weldment of UNS 31803 was made in three passes and in between the successive passes, a time of cooling of 120 seconds was allowed. Nine welding conditions were given as weldments were produced at different welding parameters. To ensure reliability and validity, each welding conditions were given at different weldments. See Table 3 showing the welding parameters used during welding process.

**Table 3: Welding Parameters used during Welding Process**

Parameters	Values	Units
Arc voltage V	10-12	V
Welding speed, S	50 -90	mm/min
Welding current, I	100 – 150	A
Root gap	2.0	Mm
Gas flow rate	15	L/min
Root face	1.5	Mm
Groove design	Single v-groove	
Groove angle	65 <sup>0</sup>	
Shielding gas	98%Ar + 2%N	

It is worthy to note that, before welding it is very necessary to clean the base material surface and edges of groove properly so as to remove dust, rust, oil, dirt and particles that are not wanted, otherwise defects may develop in the weld pool.



After welding, liquid penetrant examination was carried out on welding pipe to ensure no surface defect. Also, a radiographic examination was carried out to ensure no defect throughout the thickness of the pipe. Corrosion and mechanical tests were performed on the specimen according to the required standard.

### 2.2.1 Corrosion Test

Welded sample pitting behavior studies was done using ASTM G48 standard. For this test, specimen was cut into 40x20mm size after welding, and weighed using the digital weighing machine. Specimen was immersed in 100g of ferric chloride on 900ml of de-ionized water for 24hrs at a test temperature that is constant at  $(22 \pm 1) ^\circ\text{C}$  and  $(28 \pm 1) ^\circ\text{C}$ . Magnesium oxide paste was used in cleaning the specimen, rinsed well with water, dipped in acetone and air dried. Specimen was subsequently examined if there are visible pits and weighed so as to get the weight loss as a result of corrosion attack.

### 2.2.2 Metallography

Optical microscopy was used in performing the metallographic studies. Specimen was polished with A120 Abrasive grit up to 1200 grit fineness. Alumina powder of  $0.05\mu\text{m}$  size was used to carry out the cloth polishing of sample. The weldment was etched with 22% NaOH solution and examination was under optical microscope. The measure of the content of ferrite was carried out by point count method according to standard.

### 2.2.3 Mechanical Test

- i. **Hardness Test:** Vickers hardness tester was used in performing the micro-hardness test on the weldment. The measurements of hardness were taken on the weldments transverse section where measurements of values were at weld metal, base metal and HAZ.

Measurement of hardness was also along the weldments thickness. 100g load was used for the indentations with dwell time of 10s, with a gap of about 3mm in-between indentations.

- ii. **Tensile Test:** The material thickness and width for this test was 5.54mm and 14.10mm respectively. The ASME 9 standard was followed in this tensile test. The average of 3 value of test performed was used in this study.
- iii. **Impact Test:** For this test, the specimen dimension used was  $5 \times 10 \times 50\text{mm}$ . The pendulum type impact tester was used to carry out a Charpy V-notch impact test, according to ASTM A370 standard.

## 2.3 Analytical Method

### 2.3.1 Design of Experiment (DOE)

This is a method that systematically determines the connection between factors affecting a process and the process output. Experimental data are commonly analyzed using this technique. In order to optimize the output of a process, the information obtained from this analysis is required or needed to manage process inputs. It is an empirical statistical technique used for the analysis of multiple regressions using quantitative data obtained from experiments that are properly designed to solve multivariate equations simultaneously. It is a formal structured technique for studying any situation that involves a response that varies as a function of one or more independent variables and commonly used to address complex problems where more than one variable may affect a response and two or more variables may interact with each other (Kumar & Vaseem, 2018).

Figure 2 shows the flow diagram of the step by step approach for the study.

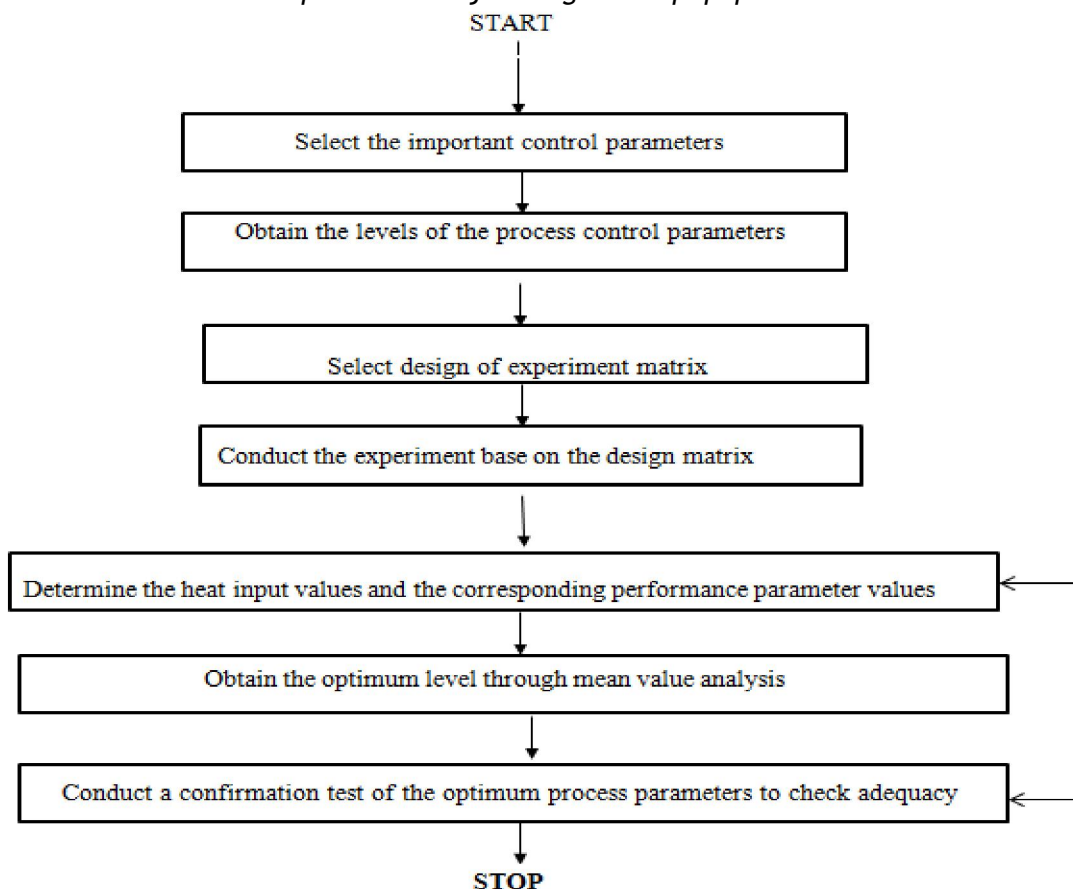


Figure 2: Flow Diagram of the step-by-step approach of the study

### 2.3.2 Taguchy Method

The Taguchy method is a systematic application of design and analysis of experiments for the purpose of designing and improving production quality. The use of a special set of arrays known as the orthogonal arrays is applied in this method. The conduction of the minimal number of experiments which could give the full information of all the factors that affect the performance parameters are stipulated by these standard arrays. Orthogonality implies that the

influence of one factor doesn't interfere with the estimation of the other factors influence and that each factor is evaluated independently (Ross & Taguchi, 1988; Wang & Northwood, 2008; Magudeeswaran *et al.*, 2014).

### 2.3.3 Selection of Orthogonal Array (OA)

The objectives of this study were considered during selection of parameters. Each parameter was analysed at three levels. See Table 4.

Table 4: Factors and Level used for the Orthogonal Array

Factors	Unit	Code	Level 1	Level 2	Level 3
Weld current	A	A	100.00	125.00	150.00
Weld voltage	V	B	10.00	11.00	12.00
Welding speed	mm/min	C	50	70	90

The degree of freedom (DOF) for each of the three level parameters is 2 (i.e., number of levels – 1). The total DOF for the 3 level of the 3 parameters each = 4 x (No of level – 1) = 4 x (3 -1) = 4 x 2 = 8. Therefore, the total degree of freedom required for the experimentation is eight (8).

The total DOF of the orthogonal array, according to the Taguchi’s method, must be greater than or equal to the experimentation total DOF needed.

A standard three level L<sub>9</sub> orthogonal array with 8 DOF  $N_{Taguchi} = 1 + \sum_{CI}^{NV} (L_i - 1)$  (i.e., 9 – 1 = 8) was selected for this study using the Taguchi based experimental design. Table 5 shows a 3 level of 9 experimental orthogonal arrays.

**Table 5: L<sub>9</sub> (3<sup>3</sup>) Orthogonal Array**

Run	A	B	C	Performance parameter value
1	1	1	1	P <sub>1</sub>
2	1	2	2	P <sub>2</sub>
3	1	3	3	P <sub>3</sub>
4	2	1	2	P <sub>4</sub>
5	2	2	3	P <sub>5</sub>
6	2	3	1	P <sub>6</sub>
7	3	1	3	P <sub>7</sub>
8	3	2	1	P <sub>8</sub>
9	3	3	2	P <sub>9</sub>

### 2.3.4 Mean Value of Each Level

The mean value of each level, j of a particular variable, i is calculated by summing the performance parameters pertaining to an individual level (see equation (2) ),

$$\text{Mean value, } \mu_{ij} = \frac{\text{Sum of the parameter of individual level of a particular variable}}{\text{The number of level}} \quad (2)$$

## 3. RESULTS

### 3.1 Welding Quality

A suitable welding current for the specimen was set up to be within 100A to 150A. Current higher than 150A with slower speed rate produces excessive heat impact and instead of welding of base metal, melting was observed. Also currents below 100A with a higher speed rate produces poorly formed weld joint due to incomplete weld penetration. The indication is that the heat input per unit length of weld obtained at a range of speed utilized in this work and current below 100A is not enough to give full weld penetration (see figure 3).



**Figure 3: Image of Welded Samples used in the Experiment**

### 3.2 Weld Microstructure

The weld root region has high formation of austenite than at the cap. This is so because during weld passes, weld root regions were subjected to reheat, hence favouring the acicular and intra-granular type of secondary austenite at the root.

At the weld cap region, the coarse ferrite grain was observed. It was noticed during welding that with increased heat input and slower rate of cooling there is higher austenite content and large grain size in the weldment. Similarly, with decreased heat input and

higher rate of cooling, there is a lower austenite content with finer grains on the weldment.

The content of ferrite at the weld cap is higher than that of the root region. Increase in grain size was observed at the HAZ region due to recrystallization of the ferrite, and the austenite formation was evident. See figure 4 showing the microstructure of welded joint heat affected zone.

The volume fraction of ferrite in the HAZ is higher than that of the welded region.

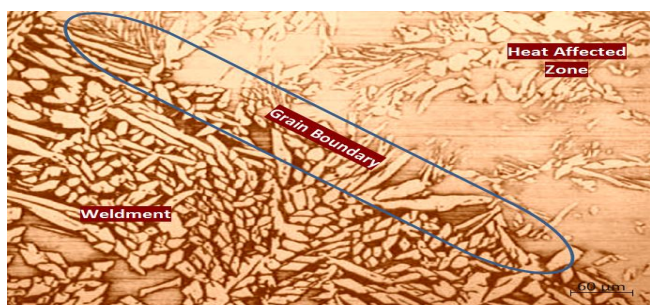


Figure 4: Microstructure of the Heat Affected Zone of welded joint

### 3.3 Results of Corrosion Test

#### 3.3.1 ASTM G48 Test

It was discovered from the obtained results that the rate of corrosion of the sample increases as heat input increases. This is due to the intermetallic phase formation like the secondary austenite which consists of a very low amount of Chromium, Cr and Molybdenum, Mo at high heat input, and this result to easy breakdown of the passive film.

Pitting was not evident at 22<sup>o</sup>C. That is, at 22<sup>o</sup>C weight loss was less than 1g/m<sup>2</sup> per day. Pitting was observed at 28<sup>o</sup>C in accordance with ASTM G48 standard which states that pitting is said to be initiated when weight loss is more than 1g/m<sup>2</sup> per day. See Figure 5 showing the variation of corrosion rate with heat input.

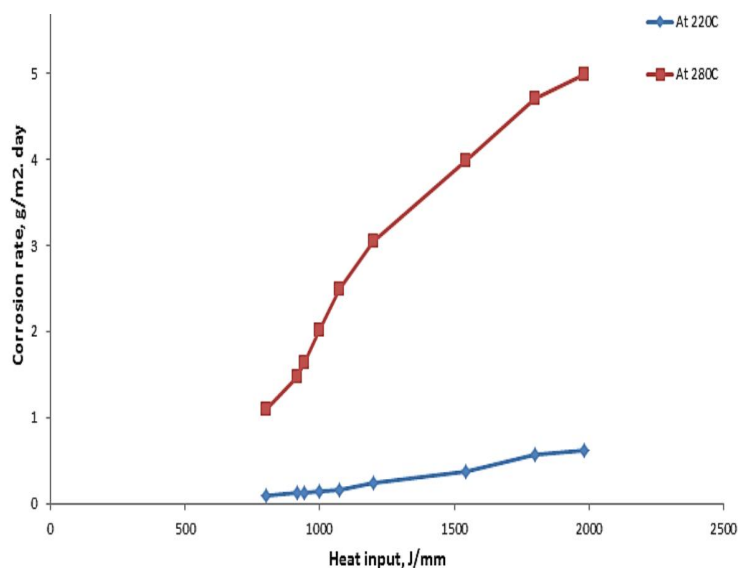


Figure 5 Corrosion rate variation with heat input

#### 3.3.2 Potentiostatic Measurement

The potentiostatic measurement was carried out to determine the Critical Pitting Temperature (CPT) in order to verify the maximum working temperature for the weldment. The Critical Pitting Temperature is the temperature at which current density of corrosion gets to 100  $\mu\text{A}/\text{cm}^2$ . It was observed that there was stable pitting between temperatures 23<sup>o</sup>C and 27<sup>o</sup>C.

### 3.4 Mechanical Test Results for Weldment

#### 3.4.1 Hardness

As a result of repeated heating and cooling, and high filler wire elements, the hardness of the base metal was found to be lower than that of the weldment. Higher hardness values were noted at low heat input and a high rate of cooling. The values of hardness were measured along the weld regions vertical line and across the transvers section of the weldment. Welded region seems to exhibit higher hardness across the transvers section than HAZ due to refinement of grain and higher alloying element. Along the vertical line, due to grain refinement and



repeated heating and rate of cooling, high hardness values were noticed at the weld root region. Because the rate of cooling of surface weld is faster than the inside, the hardness of the weld cap was observed to be lower than the root but higher than the center of weld. See Table 6 showing  $L_9$  Orthogonal array for hardness test and experimental results.

**Table 6:  $L_9$  Orthogonal array for hardness test and experimental results**

Run	Current, A	Voltage, V	Speed, mm/min	Heat input J/mm	Hardness, HVN			
					X <sub>1</sub>	X <sub>2</sub>	X <sub>3</sub>	Mean
1	85	10	50	1200.00	266	270	273	269.67
2	85	11	70	942.86	310	312	310	310.67
3	85	12	90	800.00	350	354	360	354.67
4	115	10	70	1071.43	275	270	273	272.67
5	115	11	90	916.67	320	315	317	317.33
6	115	12	50	1800.00	205	195	195	198.33
7	150	10	90	1000.00	290	300	288	292.67
8	150	11	70	1980.00	170	183	188	180.33
9	150	12	50	1542.86	212	215	222	216.33

### 3.4.2 Tensile Strength

The parent metal showed lower strength values compared to the weldment. This is as a result of the high tensile strength filler metal properties. 916 MPa was the obtained highest strength. Fracture occurred outside the welded region. From the result, it was observed that due to higher rate of cooling induced in

welds of low heat input, low heat input leads to higher tensile strength, which also leads to finer grain size and more formation of ferrite as compared to higher heat input. See Table 7  $L_9$  Orthogonal Array for Tensile Test and Experimental Results.

**Table 7:  $L_9$  Orthogonal Array for Tensile Test and Experimental Results**

Run	Current, A	Voltage, V	Speed mm/min	Heat input J/mm	Tensile strength, MPa
1	100	10	50	1200.00	805
2	100	11	70	942.86	833
3	100	12	90	800.00	916
4	125	10	70	1071.43	820
5	125	11	90	916.67	859
6	125	12	50	1800.00	712
7	150	10	90	1,000.00	817
8	150	11	50	1980.00	653
9	150	12	70	1542.86	737



### 3.4.3 Impact Toughness

Factors like intermetallic phase, grain size, austenite formation, etc. can affect the impact toughness of a material (Paulraj & Garg, 2015).

Due to slow cooling resulting to the coarse grain formation, it was observed that toughness value of weldment reduces because of high heat input. As shown in table 7, precipitation of intermetallic phase is unavoidable at high heat input, and may lead to reduced impact toughness properties of the weld,

though high heat input also facilitates austenite formation.

The impact value varies at various regions from the base material to the weld center line. The V-notch was made at various points, at fusion line, weld metal, 2mm and 5mm from fusion line for proper understanding of the test values. Low impact toughness values at fusion line were observed as compared to the weld center. The observation at positions 2mm and 5mm was that toughness values were high.

**Table 8: L<sub>9</sub> Orthogonal array for toughness test of weldment and the experimental results**

Run	Current, A	Voltage, V	Speed mm/min	Heat input, J/mm	Impact Toughness, J
1	85	10	50	1200	169
2	85	11	70	942.86	188
3	85	12	90	800	203
4	115	10	70	1071.43	172
5	115	11	90	916.67	197
6	115	12	50	1800	108
7	150	10	90	1000	175
8	150	11	70	1980	98
9	150	12	50	1542.86	110

### 3.5 Calculation of the Mean Value, $\bar{\mu}$ of Each Level

The calculation of the mean values of a particular variable of each level is carried out as stated in equation 2.

The calculation of the mean value for each control factor was done in order to evaluate the effect of each selected factor on the responses.

**Table 9: ANOM for Calculated Hardness Mean Values**

Factors	Current, A (A)	Voltage, V (B)	Speed, mm/min (C)
Level 1	311.67	278.34	216.11
Level 2	262.77	269.44	266.56
Level 3	229.77	256.44	321.56
Range	81.90	21.90	105.45
Rank	2	3	1

**Table 10: ANOM for calculated tensile strength mean values**

Factors	Current, A A	Voltage, V B	Speed, mm/min C
Level 1	851.33	814.00	723.33
Level 2	797.00	781.67	796.67
Level 3	735.67	788.33	864.00
Range	115.66	32.33	140.67
Rank	2	3	1

**Table 11: ANOM for Calculated Impact Toughness Mean Values**

Factors	Current, A (A)	Voltage, V (B)	Speed, mm/min (C)
Level 1	186.67	172.00	125.00
Level 2	159.00	161.00	156.67
Level 3	127.67	140.33	191.67
Range	59.00	31.67	66.67
Rank	2	3	1

As shown in Tables 8, 9 and 10, welding speed has the most effective influence on the quality of properties of the weldment. The optimized parameter for tensile strength, hardness and toughness were  $A_1 = 100A$ ,  $B_1 = 10V$  and  $C_3 = 90\text{mm/min}$ . These parameters were used to perform a confirmation experiment that resulted to the tensile, hardness, and impact toughness values.

Heat input range recommended for this grade of stainless steel undergoing the GTAW process is  $0.5 - 2.5\text{kJ/mm}$ . In this study, the optimized parameters of the GTAW process gave a heat input of  $0.667\text{kJ/mm}$  which falls within the range recommended, and the corresponding values of tensile strength, hardness and impact toughness were recorded as  $994\text{MPa}$ ,  $371\text{HVN}$  and  $237\text{J}$  respectively. The corrosion test performed at  $22^\circ\text{C}$  and  $28^\circ\text{C}$  had no trace of corrosion on the weldment  $0.04\text{ g/m}^2\text{ day}$  and  $0.74\text{g/m}^2\text{ day}$

respectively, which is below the  $1\text{g/m}^2\text{ day}$  in which corrosion is said to be initiated.

#### 4. CONCLUSION:

Performance of the welding process of Gas Tungsten Arc Weld on UNS S31803 stainless steel pipe was successful. Due to multiple heating cycles, the hazardous secondary austenite precipitation in the root of the weld arises, and this causes more susceptibility to pitting attack of the weld region as compared to the weld cap region. It was discovered from the experiment conducted that low heat input weld gives a better resistance to corrosion and mechanical properties than welding with higher heat input.

The optimum welding parameters of the experiment were found to be  $100A$ ,  $10V$ ,  $90\text{mm/min}$  for welding current, voltage, and speed respectively. It was observed from the Critical Pitting Temperature that there was occurrence of critical pitting between  $23^\circ\text{C}$  and  $27^\circ\text{C}$ . The corrosion rate for the optimized parameters, at  $22^\circ\text{C}$  and  $28^\circ\text{C}$  were  $0.04\text{g/m}^2\cdot\text{day}$  and  $0.74\text{g/m}^2\cdot\text{day}$  respectively, which is lower than the  $1\text{g/m}^2\cdot\text{day}$  in which corrosion is said to be initiated.

High heat input decreases the hardness values of UNS S31803 stainless steel. Due to varying thermal cycles, weld root region values of hardness were observed to be high. The hardness value for the optimized parameters was  $371\text{HVN}$ . From the experiments conducted, it was found that the tensile strength of weldment was higher than the base material. The optimized parameters have a tensile strength of  $994\text{MPa}$ . It was found that increasing the heat input decreases the tensile strength of UNS S31803 stainless steel.

Impact toughness of the stainless-steel weldment increases as heat input decreases due to increase in the size of grain, formation of intermetallic phase, and the formation of secondary austenite at high heat input.



The impact toughness for the optimized parameters of this study was 237J. The contribution to knowledge of this study is that, based on the mean value analysis calculated, it has been found that welding speed has the most effective influence on the quality of properties of the weldment over welding current and welding voltage, where other process parameters are unaltered. Generally, careful control of the welding parameters increases the mechanical properties and resistance to corrosion of UNS S31803 stainless steel weldment, and this can be achieved by proper optimization of the parameters.

## REFERENCES

- Abioye, T. E. (2017). The Effect of Heat Input on The Mechanical and Corrosion Properties of Aisi 304 Electric Arc Weldments. *British Journal of Applied Science and Technology*. 20 (5). 1 – 10.
- ASTM G48 Standard Test Method for Pitting and Crevice Corrosion Resistance of Stainless Steels. Retrieved from <https://www.corrosionguru.com/astm-g48-pitting-resistance-testing/>
- Davis, J.R. (2006). Corrosion of Weldments. *Materials Park*. ASM International. OH, USA.
- Elena, B. (2014). Analysis of Corrosion Resistance Property of Cold Bended 316L and 6M<sub>0</sub> Stainless Steel Pipes. (Master's Thesis). University of Stavanger, Norway.
- Funderburk, R.S. (1999). A Look at Heat Input. *Welding Innovation*. 16(1), 8 – 11.
- Handbook for Analytical Methods for Materials. (2009). Electrochemical Corrosion Testing. Retrieved from <http://mee-inc.com/esca.html>. <http://www.ecs.umass.edu/mie/labs/mda/fea/sanka/cha p5.html>
- Hynn, J., Shin, T., Kin, S., & Koh, J. (2017). A Study on Characteristics of Duplex Stainless Steel (ASTM A240 UNS S31803) Weld Metals Made with Fcaw. *Journal of Welding and Joining*. 35 (4), 74 – 81.
- Kumar, M., & Vaseem, M. (2018). Effect of SiO<sub>2</sub> in an A-GTAW made of AISI SS304. *International Journal of Advance Engineering and Research Development*. 5 (3), 2348 – 6404
- Magudeeswaran, G., Nair S.R., Sundar, L., & Harikannan, N. (2014). Optimization of Process Parameters of the Activated Tungsten Inert Gas Welding for Aspect Ratio of UNS32205 Duplex Stainless-Steel Welds. *Defense Technology*. 10 (3), 251 - 260.
- Manapparai, M., & Elango, A. (2016). Taguchy Based Optimization of TIG Welding Parameters on AISI310 and 321 Grade Austenitic Stainless Steel. *Journal of Production Engineering*. 19 (1), 87 – 90.
- Marcus, P., (Ed.). (2002). Sulphur-assisted Corrosion Mechanisms and the Role of Alloyed Elements. *Corrosion Mechanisms in Theory and Practice*, (2<sup>nd</sup> ed.). Merceel Dekker, NY.
- Pardal, J.M., Souza, G.C., Tavares, S., Cindra, F. M., Ferreira, M., Martins, L. & Filho, O. (2011). Characterization and Evaluation of Corrosion Resistance of Welded Joint of Duplex Stainless-Steel Pipe UNS S31803 by Submerged Arc Process. *Soldagem & Inspecao*. 16, 310 – 321.
- Paulraj, P., & Garg, R. (2015). Effect of Welding Parameters on Mechanical Properties of GTAW of UNS31803 and UNS32750 Weldments. *Manufacturing review*. 2, 29.
- Paulraj, P., & Garg, R. (2016). Effect of Welding Parameters on Pitting Behaviour of GTAW of DSS and Super DSS Weldments. *Engineering Science and Technology, an International Journal*. 19 (2), 1076 – 1083.



- Potapov, N.N. (1993). Oxygen Effect on Low – Alloy Steel Weld Metal Properties. *Welding Journal*. 72 (8) 367s – 370s.
- Ross, P., & Taguchi, J. (1988). Techniques for Quality Engineering. *McGraw-Hill International Edition*. New York. USA
- Singh, G. (2018). A Simple Introduction to Anova (with Application in Excel). <http://www.analyticsvidhya.com/blog/2018/01/anova-analysis-of-variance/>
- Trethewey, K.R., & Chamberlain, J. (1995). Corrosion for Science and Engineering (2<sup>nd</sup> ed.). Essex, England. Addison Wesley Longman.
- Verma, J., Taiwade, R.V., Kataria, R., Kanishka, J., & Vipin, T. (2019). Evolution of Metallurgical Phases and its Co-Relation with Mechanical Properties and Corrosion Resistance of 22Cr-5Ni – 3M<sub>o</sub> and 16Cr – 10Ni – 2M<sub>o</sub> Dissimilar Weldments. *Metallography, Microstructure and Analysis*. 8 (4), 506 – 516.
- Wang, Y., & Northwood, D.O. (2008). Optimization of the Polypyrrole - Coating Parameters for Proton Exchange Membrane Fuel Cell Bipolar Plates using the Taguchi Method. *Journal Power Sources*. 185 (1), 226 - 232.
- Welding Handbook, Vol. 1 (7th ed.). (1976). America Welding Society, Miami, FL.
- Welding Handbook, Vol. 2 (7th ed.). (1978). America Welding Society, Miami, FL.
- Zhang, Z., Jing, H., Hu, L., Han, Y., Zhao, L., Xiaoging, L., & Zhang, J. (2018). Influence of Heat Input in Electron Beam Process on Microstructure and Properties of Duplex Stainless-Steel Welded Interface. *Applied Surface Science*. 435, 352 – 366.